

Advanced 3D printed mini-vascular network for self-healing concrete

Cristina De Nardi^{a,*}, Diane Gardner^a, Davide Cristofori^b, Lucio Ronchin^c, Andrea Vavasori^c, Tony Jefferson^a

^a Resilient Structures and Construction Materials (RESCOM) Research Group, School of Engineering, Cardiff University, Queen's Buildings, The Parade, Cardiff, CF243AA Wales, United Kingdom

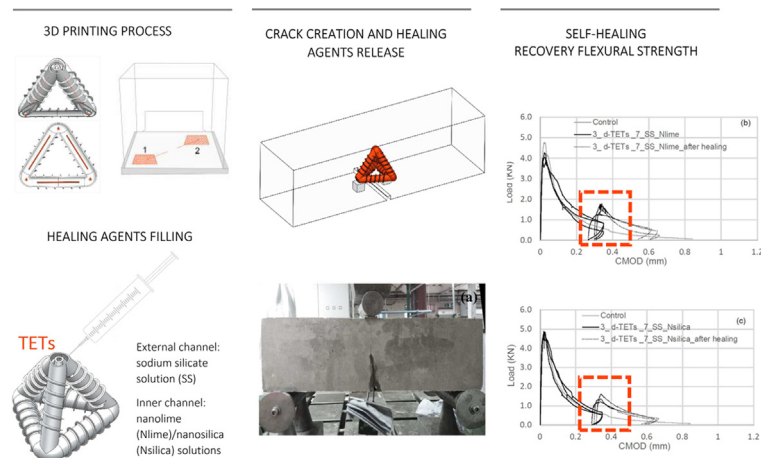
^b Centre for Electron Microscopy "Giovanni Stevanato" and Department of Molecular Sciences and Nano Systems, Ca' Foscari University of Venice, Venice, Italy

^c Department of Molecular Sciences and Nano Systems, Ca' Foscari University of Venice, Venice, Italy

HIGHLIGHTS

- 3D printed d-TETs satisfied the requirements, i.e. impermeability, rupture and release of healing agents at intended crack width.
- The coaxial dual channels provide an effective system for supplying bi-component healing agents.
- Strength and stiffness recoveries following 3-point bend tests after healing showed ceiling values of 25% and 40% respectively.
- A certain modification to the PLA polymer structure has been observed when in contact with the alkaline healing agents.

GRAPHICAL ABSTRACT



ARTICLE INFO

Article history:

Received 13 September 2022

Revised 17 December 2022

Accepted 16 April 2023

Available online 19 April 2023

Keywords:

3d printing

Self-healing concrete

Mini-vascular networks

Biomimetic structures

Bi-component healing agent

ABSTRACT

Recently, the development of 3D mini-vascular networks has demonstrated their ability to facilitate self-healing in concrete structures. These 3D printed polylactide (PLA) hollow ligament tetrahedral shaped units (TETs) can heal multiple occurrences of damage by releasing a single-component healing agent stored within. To improve the healing efficacy of the concrete-TET system whilst overcoming the potentially short shelf life of single-component healing agents, the TETs design was modified. TETs with coaxial hollow ligaments (d-TETs) suitable for storing bi-component healing agents were manufactured. Different healing agents, including epoxy resin (i.e. cycloaliphatic epoxy resin plus hardener) and sodium silicate in isolation or in combination with either nanosilica or nanolime solution were explored. The d-TETs were effective in storing these bi-component healing agents without them undergoing premature mixing and curing. Moreover, the d-TETs successfully ruptured and released healing agents at a crack width of 0.35 mm. After one damage-healing cycle, significant strength and stiffness recovery was achieved: d-TETs hosting sodium silicate and nano-lime yielded the best strength recovery (25%), whilst most other sodium silicate-based healing agent combinations demonstrated stiffness recoveries of approximately 40%. This demonstrates the efficiency of the d-TETs concept as a system, which allows strength and stiffness recovery despite the limited volume of healing agent.

© 2023 The Authors. Published by Elsevier Ltd. This is an open access article under the CC BY license (<http://creativecommons.org/licenses/by/4.0/>).

* Corresponding author.

E-mail address: denardic@cardiff.ac.uk (C. De Nardi).

1. Introduction

Biomimicry is one of a series of novel approaches being adopted in civil engineering to meet the growing demand for construction materials with improved and extended service-life performance [1,2]. The latter is achieved by enhancing the material's durability by making it aware of, and able to respond to, damage, which minimizes or even eliminates the need for ongoing repair and/or material replacement interventions [3,4,5].

In the last two decades, autogenic (natural) and autonomic (engineered) healing techniques have been studied. Cementitious materials undergo autogenic healing upon exposure to moisture, resulting in partial or total self-closure of cracks, as well as partial recovery of initial durability and physical–mechanical properties [6,7]. It was proven that by combining continued hydration and carbonation processes (i.e. autogenous healing), under ideal curing conditions, cement-based construction materials have an inherent ability to heal cracks up to 0.15 mm [8].

A variety of functionally engineered cementitious systems have been developed to enable larger and more complex systems of cracks to self-heal [9–10]. In this respect, the vascular healing concept in concrete takes a biomimetic approach to self-healing, by mimicking the human cardiovascular system that transports blood, and hence healing agents, around the body and the plant vascular tissue system.

In the last three decades, liquid-based self-healing systems for cementitious materials have been developed, based on the concept of the release of limited quantities of stored healing agent from brittle macro-sized tubes [4,5,11,12] – or from polymer microcapsules [13,14,15].

Encapsulation technology is an effective method for self-healing over a wide range of crack openings, i.e. 5–400 μm [16]; however, it usually precludes repeated damage repair, since the supply of healing agent is often fully exhausted in the first damage event. Many factors might affect the performance of self-healing concrete containing capsules, such as the capsule material [17,18,19], the composition and nature of the healing agent [20,21], and the crack configuration and morphology [22,23]. To overcome some of these challenges, the use of a continuous biomimetic vascular network, as first presented by Dry [12], has been proposed to provide an advanced approach for liquid-based self-healing.

Vascular network systems allow the healing agent to be distributed under low pressure from an external reservoir to the damage location [24], and offers the potential to supply different healing agents over different temporal scales in response to varying damage scenarios [25]. The main strategies adopted in recent years concern the creation of channels through a variety of methods, such as the embedment of tubes/pipes in the concrete matrix [23,26,27], the formation of hollow channels via the removal of smooth pipes [12,28], or the insertion of 3D printed vascular networks [29,30]. Joseph et al [31] embedded four hollow brittle glass tubes into mortar beams: the tubes were open to the atmosphere and filled with a single-component cyanoacrylate (CA). The authors demonstrated that a low viscosity cyanoacrylate adhesive offered the greatest chance of flowing into the crack, providing a successful mechanism for restoring the mechanical properties of the mortar specimens following damage. Dry et al. [32,33] studied structural scale elements, i.e. continuous bridge deck slabs containing encapsulated healing agent and a small concrete frame with embedded hollow glass tubes. The authors demonstrated that the strengths of samples increased after full curing of the adhesives (10 days after damage).

Pareek et al [28] developed a self-repairing system for reinforced concrete by using a network system. The hollow channels were filled with epoxy resin injected with a syringe from the open end. A remarkable regain of flexural strength was evident in mortar

samples injected with the lower viscosity resin. To overcome the small reduction in strength caused by the presence of hollow channels within a structural member, Sangadji [34] proposed the use of prefabricated porous concrete cylinders placed in the centre of larger concrete cylinders. When damage was detected by sensors, epoxy agent stored in reservoirs was injected through the porous concrete via a pump. Mechanical tests and visual observations confirmed the successful healing performance of the system, showing strength and stiffness regain [35].

Vascular network systems of 2D and 3D configurations have been studied by a number of researchers, with a view to improving the healing performance by increasing the volume and continuity of healing agent supply. Davies et al [36] created a 2D reusable vascular network using linear interconnecting hollow channels filled with either sodium silicate solution (SS) or cyanoacrylate adhesive (CA), both supplied under low pressure. The authors highlighted that SS was easier to handle and supply into the vascular network; however, in samples containing CA the strength recovery was higher (up to 90%) than SS in a significantly shorter time. Minnebo et al [30] studied a vascular system that was formed by tubes connected to a 3D printed distribution piece. The polyurethane (PU) used as healing agent was successfully injected into the piping system when a crack occurred. The degree mechanical recovery was measured over three damage-healing cycles and the ability of the system to achieve repeated healing was demonstrated. A biomimetic three-dimensional 3D printed vascular network was designed by Li et al [29], the authors underlined that the presence of the plastic tubes act as reinforcement within the cementitious beams. Following damage, recoveries in mechanical properties of $\sim 20\%$ for 1D and 2D and up to 34% in 3D vascular networks were reported. The efficiency of various healing agents for use in cementitious materials has been widely studied, although much of the work has focused on mono-component healing agents such as CA [17,37,38], epoxy resins [28,39], SS [21], and PU [40,41]. Generally, mono-component agents are preferred for their good flow properties; however, an unavoidable shortcoming is their limited shelf life. The use of CA adhesives has also proven challenging for the scaling-up of self-healing systems, owing to difficulties associated with handling large volumes of highly reactive adhesive, coupled with their propensity to undergo premature curing whilst encapsulated. Recently, new formulations of CA have been explored with the aim of retarding its curing rate, improving its stability and reducing the amount of premature hardening that occurs during the encapsulation period. The latter is important because premature hardening is associated with the formation of network blockages. Several studies have focused on the potential for silicates and alkali silica solutions to act as healing compounds in cement-based composites [32,42] and in recent years aqueous sodium silicate has been widely used to form the core of microencapsulated systems [15,21,43,44,45].

A number of studies that have used multi-component healing agents have also been reported in the literature: these include, studies on the use of a two-compound epoxy resin [32] and a multi-compound methyl methacrylate (MMA) system [12,20]. These showed that they can be fully activated in situ, at the damage location, only if appropriate proportioning and mixing between the two-compound parts can be achieved. However, despite all the encouraging laboratory results from the studies highlighted above [46], the achievement of full-scale vascular networks in concrete structures remains an ongoing challenge, not least because of anticipated delays to the concrete casting process resulting from the in-situ placement of the vascular networks.

In response to these concerns, researchers at Cardiff University have recently developed mini-vascular networks (MVNs), as an alternative to conventional vascular networks. The MVNs used in the present work comprise 3D tetrahedral units with hollow liga-

ments, called TETs [47]. The design is based on the idea that any crack plane will fracture multiple ligaments by crossing the TETs between the apices. This prevents the build-up of negative pressures, which were observed by Joseph et al [27] to hinder the release of the healing agent when encapsulated in tubular capsules. Mimicking the blood circulation system, TETs act as discrete reservoirs that are able to store a sufficient volume of healing agent to allow for repeated damage repair [47]. Moreover, the placement of multiple TET units within a structure will enable continued healing of the host material.

In recent years, De Nardi et al [47] showed that TETs provide a convenient self-healing technology that can be easily introduced to wet concrete during the mixing process [47,48]. The TET design has been optimized to provide good bond properties with the matrix, rupture at an appropriate strain survived the concrete mixing process and release sufficient agent to heal macro-cracks. Moreover, it has been demonstrated that: i) TETs filled with SS can produce strength and stiffness recoveries of 20% and 75–80% respectively in prismatic concrete beams; and ii) TETs filled with SS can heal multiple occurrences of damage [47,48].

Given the shortcomings previously highlighted with mono-component healing agents, attention has now been directed towards the development of co-axial hollow channelled TETs (d-TETs) suitable for multi-component agents.

The aim of the work reported in this paper was to design a d-TET and determine its efficiency as a carrier of a bi-component healing agent when the d-TET was embedded within concrete specimens. Concrete prisms were tested in flexure under 3-point bending and the crack mouth opening displacement recorded. Different healing agents were studied: a commercially available bi-component epoxy resin and a SS solution combined with either a nanolime or nanosilica solution. For the sake of comparison, samples containing two single channel TETs, filled with SS and either nanolime or nanosilica solution as described in [47] were also cast.

This paper firstly presents an overview of studies conducted on the manufacture of the d-TETs, specifically the influence of the design and the printing parameters on their permeability and mechanical behaviour. It also presents the selection and justification of the healing agent and promoters used in the study. Secondly, the experimental programme, experimental procedures and materials are described. This includes a summary of the test arrangements for flexural tests on prismatic specimens and the Differential Scanning Calorimetry (DSC) analysis performed on different PLA samples. The experimental results and discussion are then presented, comprising the healing efficiencies of specimens containing d-TETs and microscopy and SEM/EDS analyses related to the nature of the hardened healing product. Characterisation of the PLA polymer from each stage of the d-TET manufacture and testing stage is also reported in order to better understand the influence of 3D printing on the polymer properties and the interaction between the polymer, encapsulated healing agent and cementitious matrix.

2. Design and materials

2.1. Dual channel TET (d-TET) design

Cardiff University researchers developed a new method for forming two-dimensional continuous vascular networks for cementitious materials, in response to the inherent weakness and 'single-use only' feature of closed-form hollow capsules. De Nardi et al [47] proposed an alternative approach, involving the insertion of mini-vascular networks (MVNs) into the cementitious matrix. These 3D tetrahedral units, so-called TETs, have solved the issue of suction within 1D tubular capsules which inhibits the

release of liquid healing agents. Moreover, as a result of the tetrahedral shape, the ligaments can be crossed by cracks more easily since they are straight between anchor points (apices), thus achieving rupture at a serviceability level crack (0.15–0.3 mm). A series of preliminary investigations was conducted to establish a successful and convenient, repeatable 3D printing process for manufacturing d-TETs for concrete structures. Starting from previous studies conducted on single channel TETs [47], the criteria for manufacturing d-TETs was that they are: i) completely watertight, avoiding chemical interactions between the healing agents and the matrix before the breakage occurrence; ii) able to rupture – both internal and external channels simultaneously – at the designed crack opening value and iii) 3D printable with an easily-repeatable and functional process. The initial stage of the d-TET development involved printing and testing three variants of a dual co-axial hollow channel tetrahedral unit. d-TETs were printed from a commercial transparent PLA (provided by Ultimaker, 2.85 mm diameter) using an Ultimaker2® printer (Utrecht, Netherlands) with a 0.25 mm nozzle and a 0.06 mm layer height. The properties of the d-TET variants are summarised in Fig. 1: a 6 mm external diameter ligament was taken as the basis for the design, since it successfully ruptured at a desired crack opening of 0.3 mm [47] whilst the dimension of the internal channel was chosen to store a commercial bi-component adhesive in the ratio 1:5 by volume [49]. Ink was used in lieu of a healing agent in this preliminary d-TET design stage, in order to gain a clear representation of channel integrity and ligament rupture.

Initial experimental observations revealed that Variant_I had leakages from the internal channels, mainly at the corners, as can be seen in Fig. 2. Moreover, the small size of the internal channel did not allow for easy injection of the ink. As a result, the design of Variant_II was adjusted as follows: (i) the channel dimensions were increased to ease injection and increase the volume of healing agent, (ii) the print speed was reduced to 40 mm/s in order to improve the accuracy of the overall printing (and hence enhance watertightness); (iii) supports between the internal and external channel were printed in the middle of the base ligaments to give additional stability during the printing of the internal channels. Nevertheless, despite these amendments, some internal leakage was still evident (see Fig. 2) at the junctions between the ligaments and the base. Finally, in Variant_III punctual (column-like) supports were added at the corners, and the wall thickness of the internal channels was increased to 0.75 mm, thereby reaching full watertightness (Fig. 2). An external scaffold structure was required to support the d-TET ligaments during the 3D printing process. In order to easily remove this scaffold structure, the material density was set to 10%. The final dimensions of the Variant_III d-TET are provided in Fig. 3.

2.2. Healing agent selection

The healing principle which underpins the MVN technology strongly relies on the timely rupture of the MVN channels, subsequent flow of healing agents into the crack location, and an adequate curing time for the healing agent. Moreover, the mechanical properties of the healing compounds, which result from the interaction between the concrete matrix and the healing agents, determine the success of the healing system.

As described in the previous section, the efficacy of silicates and alkali silica solutions to act as healing agents in cementitious matrices is well-known [42,45]. In order to evaluate a potential enhancement of healing performance when two prophylactic agents are simultaneously available at the time of damage in the vicinity of a crack, two different healing promoter candidates in combination with SS solution ($\text{Na}_2\text{O}_3\text{Si}$) were tested. The first, a nanolime (CaOH_2) alcohol solution, marked as Nanorestore® by

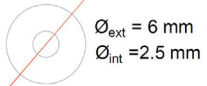
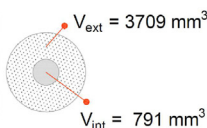

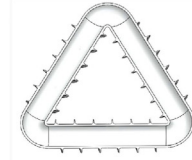
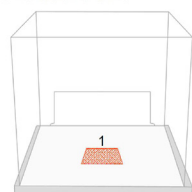
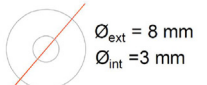
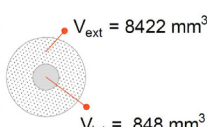
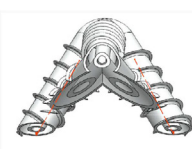
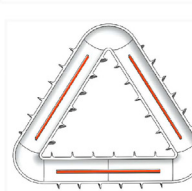
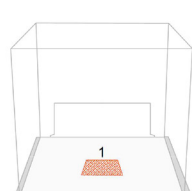
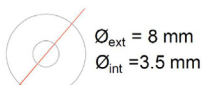
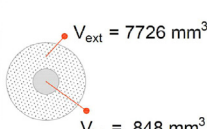
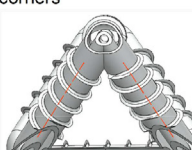
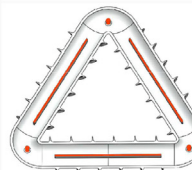
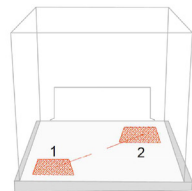
	PARTS SIZE	COMPLEXITY	PRINTING	SERIES	FUNCTIONALITY
VARIANT_I	Edge length: 42 mm Ribs: spiral, pitch 5 mm External wall thickness: 0.5 mm (0.25 x 2) Inner wall thickness: 0.25 mm  $\varnothing_{ext} = 6 \text{ mm}$ $\varnothing_{int} = 2.5 \text{ mm}$  $V_{ext} = 3709 \text{ mm}^3$ $V_{int} = 791 \text{ mm}^3$	Supports to the inner channel : NO  	PLA filament : clear Printing orientation (θ): axis x+15°; y +15° Outer wall print speed : 60 mm/sec Printing temperature: 200 °C	One at one time  Printing time: 3' 36" Material: 0.5 m	Impermeability: ext channel ✓ int channel ✗ Rupture at designed CMOD: ✓ Injection: ext channel: ✓ Int channel: ✗
VARIANT_II	Edge length: 45 mm Ribs: spiral, pitch 5 mm External wall thickness: 0.5 mm (0.25 x 2) Inner wall thickness: 0.5 mm (0.25 x 2)  $\varnothing_{ext} = 8 \text{ mm}$ $\varnothing_{int} = 3 \text{ mm}$  $V_{ext} = 8422 \text{ mm}^3$ $V_{int} = 848 \text{ mm}^3$	Supports to the inner channel : along the tube: 25 mm  	PLA filament : clear Printing orientation (θ): axis x+15°; axis y +15° Outer wall print speed : 40 mm/sec Printing temperature: 195 °C	One at one time  Printing time: 4' 28" Material: 0.6 m	Impermeability: ext channel ✓ int channel ✗ Rupture at designed CMOD: ✓ Injection: ext channel: ✓ Int channel: ✓
VARIANT_III	Edge length: 45 mm Ribs: spiral, pitch 5 mm External wall thickness: 0.5 mm (0.25 x 2) Inner wall thickness: 0.75 mm (0.25 x 3)  $\varnothing_{ext} = 8 \text{ mm}$ $\varnothing_{int} = 3.5 \text{ mm}$  $V_{ext} = 7726 \text{ mm}^3$ $V_{int} = 848 \text{ mm}^3$	Supports to the inner channel : - along the tube: 25 mm - punctual supports at the corners  	PLA filament : clear Printing orientation (θ): axis x+15°; axis y +15° Outer wall print speed : 50 mm/sec Printing temperature: 195 °C	One at one time  Printing time : 9' 48" Material: 1.15 m	Impermeability: ext channel ✓ int channel ✓ Rupture at designed CMOD: ✓ Injection: ext channel: ✓ Int channel: ✓

Fig. 1. Dual channel TETs (d-TETs) variants: size, 3D printing parameters, functionality.

the Company CTS Europe and produced by CSGI – University of Florence and the second, an aqueous colloidal system of nanosilica particles solution marked as Nanoestel[®] (by CTS Europe).

A bi-component cycloaliphatic epoxy resin, frequently employed as a structural stone strengthening agent in monuments was also tested. The mechanical behaviour of this resin was tested on different stone substrates, and it was found to have a promising performance, comparable to that of acrylic resins [50,51]. Moreover, the low viscosity of both components facilitates their release upon breakage of the d-TET ligaments.

3. Materials and methods

3.1. Mix details

The mix constituents and proportions of the concrete comprised: CEM II/A-L1 32,5R cement (562 kg/m³), 0–2 mm fine aggregate sand (562 kg/m³), 0–10 mm coarse aggregate crushed limestone (1124 kg/m³), and water (253 kg/m³). The same mix proportions, constituents and mixing protocol were used throughout the experimental programme. The dry materials (coarse aggregate,

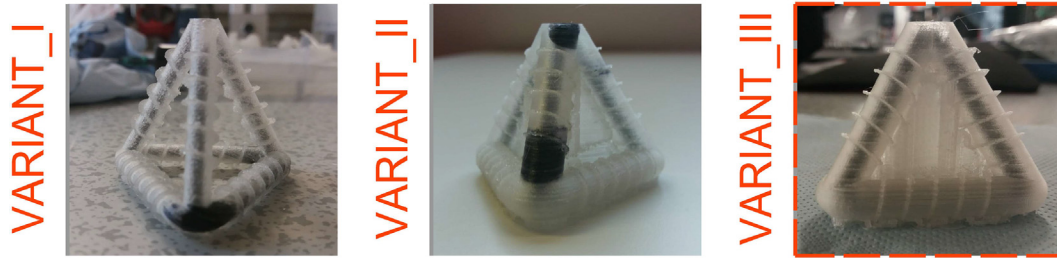


Fig. 2. Watertightness test: evidence of ink leaks in variant I and II, full watertight integrity in variant III.

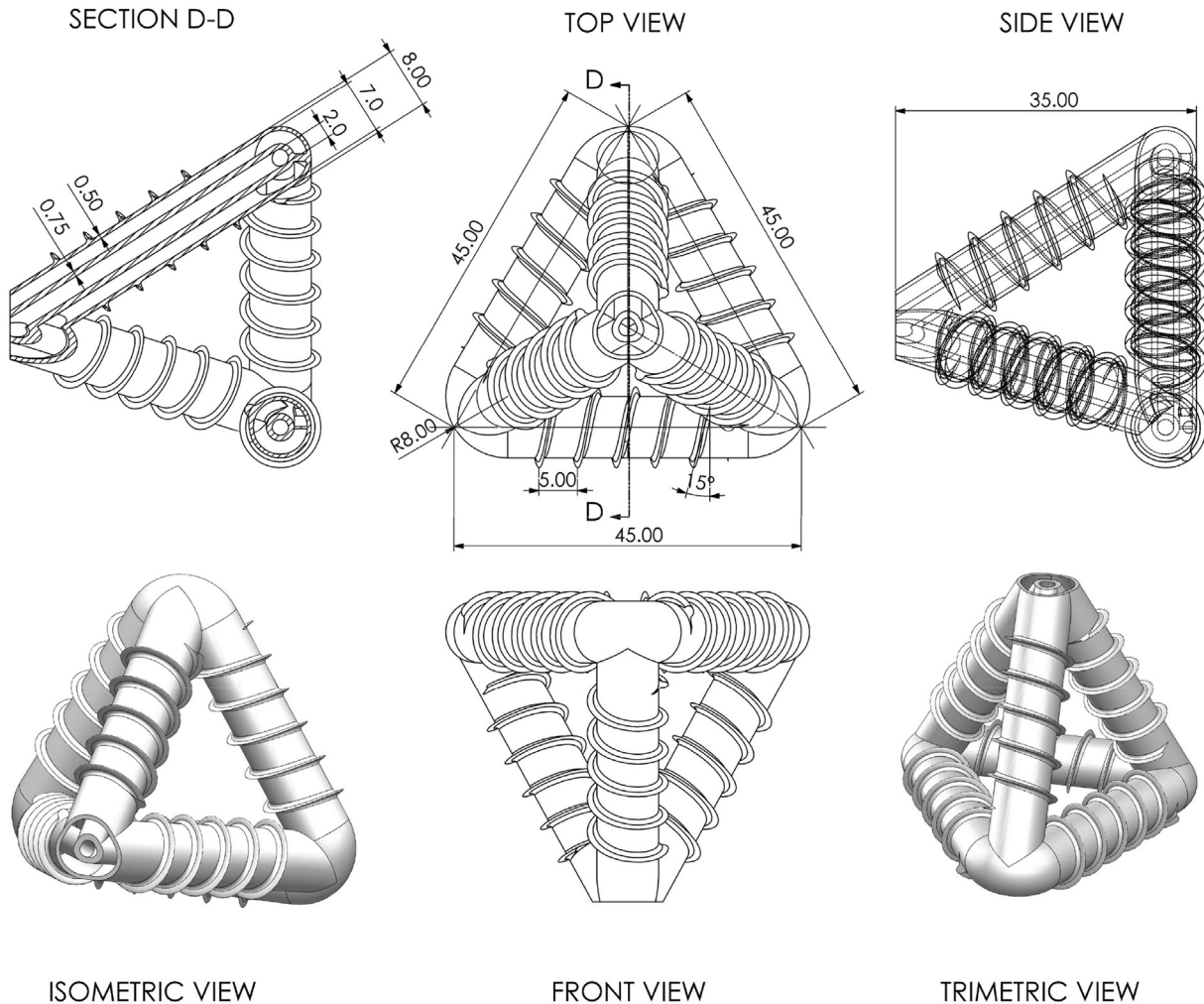


Fig. 3. Dimensions of a d-TET unit (dimensions in mm).

fine sand, cement) were mixed for 60 s, at which point the water was introduced whilst the mixer was rotating.

The moulds were filled in 3 layers, with the prism specimens filled to 10 mm from the base of the mould, allowing the d-TETs to be placed before being covered with additional concrete. d-TETs were manually placed in the centre third of a concrete prism mould (75 mm × 75 mm × 255 mm) fixed via 10 mm thickness concrete spacers secured to the bottom of the mould, as can be seen in Fig. 4 and specimens vibrated for 45 s each layer to a maximum of 45 Hz. Following 24 h of curing, the specimens were demoulded and placed in a water tank (20° C ± 5° C) for 6 days. On the 6th day a 5 mm central notch was created on the underside of the specimen in order to induce a single vertical crack during the 3-point bending testing stage.

Compression tests were conducted on three 100 mm cubes at 1, 14, 21 and 28 days in accordance with BS EN 12390-3:2009. The average compressive strength at 28 days was 48 MPa (CoV 1%). For completeness, the variation of the concrete compressive strength with time is represented in Fig. 5. After 7 days in water, ~80% of the 28-day strength had been achieved, whilst after 14 days of curing (7 days in water and 7 days in laboratory ambient conditions) ~ 95% of the compressive strength was reached.

3.2. Experimental arrangement and programme

After 7 days of curing, prisms were loaded via a 3-point bending test in accordance with BS EN 12390-5 until failure (control series) or until a crack mouth opening displacement (CMOD) of 0.35 mm

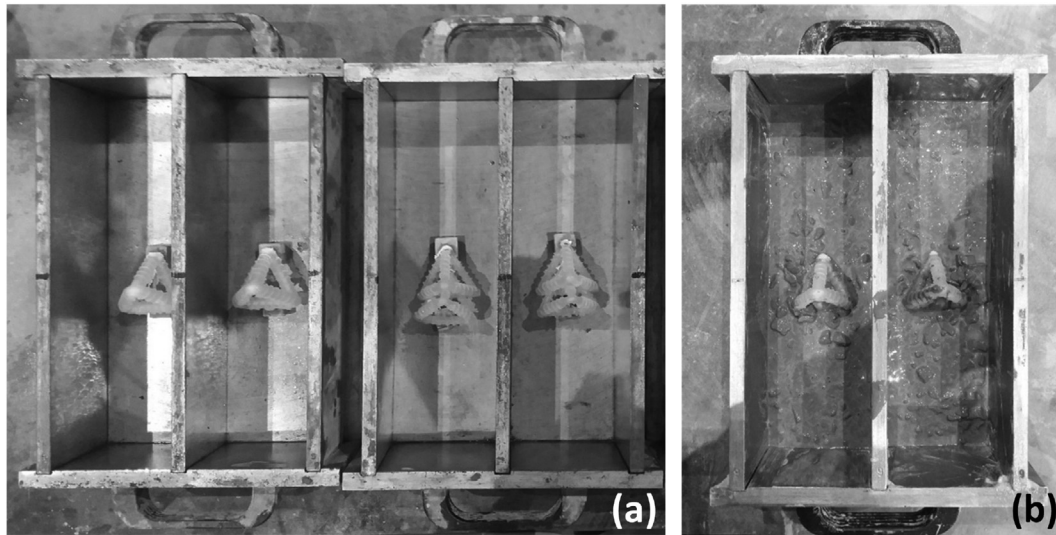


Fig. 4. (a) d-TETs position fixed via 10 mm thickness concrete spacers; (b) specimens filled to 20 mm from the base of the mould.

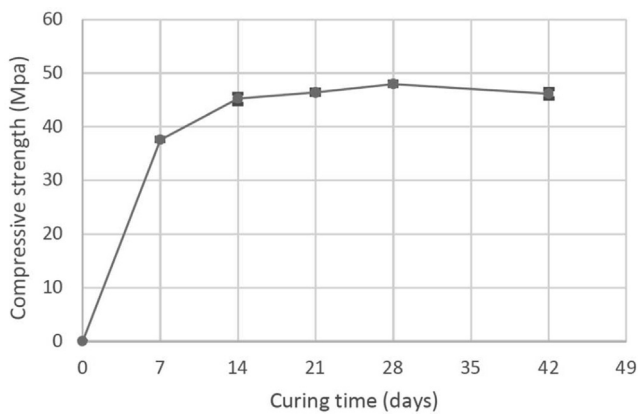


Fig. 5. Concrete compressive cube strength variation with time.

was recorded. A CMOD rate equal to 0.0001 mm/s, was used throughout the test. After the pre-cracking phase, samples were placed in laboratory environmental conditions ($20^{\circ}\text{C} \pm 5^{\circ}\text{C}$, $\text{RH} \sim 45\%$) for 14 days and then reloaded until failure. The experimental programme, as presented in Table 1, can be separated into 3 main groups. The aim of Group_1 was twofold; to explore the influence of the d-TETs on the mechanical performance of the prismatic concrete beams and to evaluate the CMOD value at which the coaxial channels forming the d-TETs' ligaments simultaneously ruptured, thus releasing both healing components. To establish the latter, samples containing d-TETs, in which only the inner channels were filled with ink, were tested under 3-point bending, during which the CMOD was held stationary for 5 min at values of 0.1 mm, 0.2 mm and 0.3 mm and any leakage of ink was noted. The Group_2 test series was undertaken to evaluate the healing potential of a range of solutions: sodium silicate (SS); nanolime (Nlime); nanosilica (Nsilica). Each solution was encapsulated within a single channel TET and combinations of these TETs were placed in concrete prisms as described by De Nardi et al. [47]. Finally, the aim of Group_3 test series was to explore the potential of d-TETs to adequately deliver the bi-component healing agents, or healing agent + promoter of healing, to zones of damage and allow sufficient reaction of the components in situ to achieve partial recovery of the undamaged flexural strength of the concrete.

Variables affecting the healing performance, such as the level of damage (i.e. crack opening up to 0.4 mm), amount of water available during the healing period, duration of healing etc, have been explored in previous studies [47]. The optimum output from that work informed the selection of variables in the current study, such as healing agent candidates, volume, CMOD value, curing/healing environmental conditions.

The sample designation is expressed as follows: V_W_X_Y; where V is the Group number; W is the type of embedded MVNs (C indicates plain concrete; d-TETs indicates MVNs with dual channels, TETs indicates MVNs with a single channel); X is the age of the first test; Y is the healing agent used to fill the MVNs (SS = sodium silicate solution, Nlime = nanolime solution, Nsilica is nanosilica solution, Epoxy = cycloaliphatic epoxy resin plus hardener). Three prismatic specimens were cast for each sample designation. In addition to the specimens detailed in Table 1, three control specimens (concrete prisms without MVNs) and three 100 mm cubes were cast and tested for each group. It should also be noted that in Group_3, SS was placed in the external channel and Nlime or Nsilica was placed in the internal channel. Similarly for the bi-component Epoxy, the hardener component was placed in the internal channel of the d-TET.

Light microscopy observations were carried out on the crack surfaces of samples containing d-TETs filled with SS and either Nlime or Nsilica (Group 3) at the end of the healing period by using a Keyence VHX-7000 digital microscope equipped with VHX-7020 high-performance camera. Fragments collected from crack surfaces were also analysed with scanning electron microscopy (SEM). The latter was carried out with a Zeiss Sigma|VP (Jena, Germany), variable pressure instrument (VP-SEM) equipped with a Bruker Quantax 200 energy dispersive x-ray spectroscopy (EDS) system (Bruker, Billerica, MA, USA).

In order to characterize the PLA polymer, Differential Scanning Calorimetry (DSC) was performed using a Linseis PTA ST1000 under nitrogen flow of 100 mL min^{-1} with a temperature ramp of $10^{\circ}\text{C min}^{-1}$ from 30 to 250°C depending on the type of measurement and polymer. Samples were collected from 3D printed d-TET ligaments; i.e. internal or external channel, before and after the contact with healing agents (and after the healing period). For completeness, DSC measurements on samples collected directly from the roll and from single channel TETs were also carried out. The experimental programme involving microscopy observations, SEM/EDS analysis and DSC is presented in Table 2.

Table 1
Experimental programme.

	Sample designation	No. units	CMOD (mm)	Ink	Healing agents				Healing period (days)
					SS	Nlime	Nsilica	Epoxy	
GROUP_1	1_C_7	0	-	-	-	-	-	-	-
	1_C_28	0	-	-	-	-	-	-	-
	1_d-TETs_7 EMPTY	1	-	-	-	-	-	-	-
	1_d-TETs_28 EMPTY	1	-	-	-	-	-	-	-
	1_d-TETs_7 INK ^{0.3}	1	0.3	✓	-	-	-	-	-
	1_d-TETs_7 INK	1	0.35	✓	-	-	-	-	-
GROUP_2	2_TETs_7_SS	2	0.35	-	✓	-	-	-	14
	2_TETs_7_Nlime	2	0.35	-	-	✓	-	-	14
	2_TETs_7_Nsilica	2	0.35	-	-	-	✓	-	14
	2_TETs_7_Nsilica_Nlime	2	0.35	-	-	✓	✓	-	14
	2_TETs_7_SS_Nlime	2	0.35	-	✓	✓	✓	-	14
	2_TETs_7_SS_Nsilica	2	0.35	-	✓	-	✓	-	14
GROUP_3	3_d-TETs_7_SS	1	0.35	-	✓	-	-	-	14
	3_d-TETs_7_SS_Nlime	1	0.35	-	✓	✓	-	-	14
	3_d-TETs_7_SS_Nsilica	1	0.35	-	✓	-	✓	-	14
	3_d-TETs_7_SS_Epoxy	1	0.35	-	-	-	-	✓	14

Table 2
Details of chemical-physical tests: microscopy, SEM/EDS analysis, DSC.

Sample tested	Microscopy	SEM/EDS analysis	DSC on PLA fragments	
			External channel	Internal channel
TET (single channel)			✓	
d-TET (dual channel)	✓		✓	✓
3_d-TETs_SS			✓	
3_d-TETs_SS_Nlime	✓	✓		✓
3_d-TETs_SS_Nsilica	✓			✓

4. Experimental results

For all specimens, their post-healing response was compared to their pre-cracking response to determine both the flexural strength and flexural stiffness healing efficacies. The nominal flexural stress is obtained from the following Equation (1), the results of the pre-cracked and post healed specimens are presented in terms of load vs CMOD responses.

$$\sigma^k = \frac{3Pl}{2bd^2} \tag{1}$$

Where P is the peak load, l is the span (200 mm), b is the width of the sample (75 mm) and d is the depth (75 mm). The results of the pre-cracked and post healed specimens are presented in terms of load vs CMOD responses. The effectiveness of healing can be evaluated by calculating the strength gained after the healing period (σ_{healed}^k) with respect to the residual strength measured at the maximum pre-cracked opening ($\sigma_{damaged}^k$) and comparing it to the maximum stress exhibited by the same specimens in undamaged conditions ($\sigma_{undamaged}^k$). The indices of strength recovery, η_{σ}^k (%) and stiffness recovery, η_K^k (%) are defined in Equation (2) and (3) respectively, with reference to the notation in Fig. 6 [52,53].

$$\eta_{\sigma}^k = \frac{\sigma_{healed}^k - \sigma_{damaged}^k}{\sigma_{undamaged}^k - \sigma_{damaged}^k} \tag{2}$$

$$\eta_K^k = \frac{K_{healed}^k - K_{damaged}^k}{K_{undamaged}^k - K_{damaged}^k} \tag{3}$$

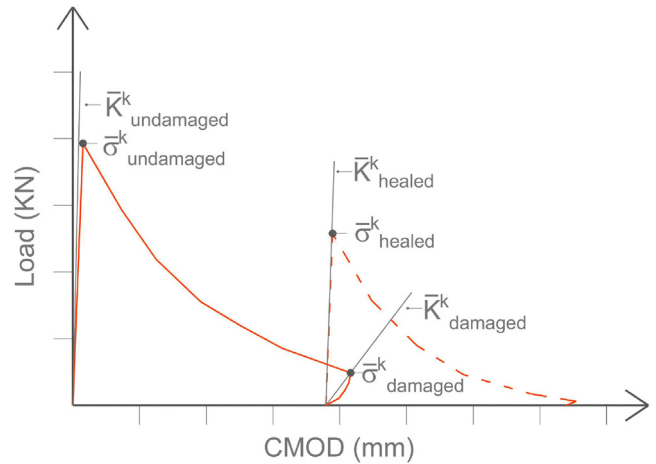


Fig. 6. Stress-CMOD curves before and after healing: notation and definition of the parameters for the indices of healing.

4.1. Group 1_Results

The flexural test results are reported in Table 3, together with indices of healing derived from the load-CMOD responses. The results shown in Table 3, are the average of three specimens.

Similarly to results previously published by the authors [47], the presence of a single d-TET within the concrete matrix reduces the flexural strength of samples tested after 7 days of curing by approximately 10%. It is worth noting that in early age samples, the presence of concrete spacers alone caused a loss in peak strength of approximately 8.5% [47].

Table 3
Group_1: Flexural test results and indices of healing.

Group_1	$\sigma_{undamaged}^{k-7}$ MPa (CoV%)	$\sigma_{damaged}^{k-7}$ MPa (CoV%)	σ_{healed}^{k-21} MPa (CoV%)	Healing efficiency		Evidence of ink release
				$\eta_{s,21}^k$ %	$\eta_{E,21}^k$ %	
1_C_7	3.8 (8)	0.37(5)	0.31(18)	0	0	
1_d-TETs_7 EMPTY	3.40 (5)	0.5(31)	0.4(29)	0	0	
1_C_28	4.75 (5)					
1_d-TETs_28 EMPTY	4.74 (6)					
1_d-TETs_7 INK ⁰³	3.5 (9)					✓
1_d-TETs_7 INK	-					✓

D-TETs are sized to allow coarse aggregate (up to 20 mm diameter) to pass through the d-TET structure, in order to minimise inhomogeneities in the matrix. Nevertheless, as highlighted for single channel TETs, poor adhesion of the matrix to either the d-TET and/or spacers particularly at early age may give rise to a small reduction in peak flexural strength. As can be seen in Fig. 7, control samples and samples containing empty d-TETs did not show any significant autogenous healing. The reinforcing effect of a d-TET, even if empty, can be seen in the flexural Load-CMOD response (Fig. 7b).

Contrary to the trend observed in the flexural strength of samples tested at 7 days, prisms with and without a d-TET cured until 28 days (7 days in water curing followed by 21 days in ambient laboratory conditions) showed almost indistinguishable flexural strength (~4.75 MPa).

With regard to d-TET breakage, it was apparent that a CMOD of 0.3 mm was sufficient to rupture the d-TET ligaments, resulting in ink release, as can be seen in Fig. 8 (a). Samples containing d-TETs, where only the inner channels were filled with ink, showed clear evidence of ink release at a CMOD equal to 0.35 mm, as can be seen in Fig. 8(b).

4.2. Group 2_Results

The results of the flexural tests performed on concrete specimens containing 2 TETs filled individually with sodium silicate solution (SS), Nanolime solution (Nlime), Nanosilica solution (Nsilica) or combinations of these three agents, are reported in Table 4.

When compared to control specimens, a marginal reduction (~12%) in flexural strength of samples containing 2 TETs filled with all healing agent candidates and tested at early age has been observed, in line with previous experimental observations [47]. When TETs are filled with Nsilica, their influence on the flexural strength is almost negligible (~6%). On the contrary, in samples containing TETs filled Nlime solution, the initial flexural strength seems to decrease further (~25%). A chemical reaction between the Nlime solution and the PLA polymer, which results in deteriora-

tion of the MVN unit, regardless of its physical form, is a plausible explanation for this reduction and one which is explored further through the differential scanning calorimetry tests.

The Load - CMOD response of Group_2 specimens can be seen in Fig. 9 (a-d). Concrete samples containing 2 TETs filled either with Nlime or Nsilica afforded a null strength recovery index, nonetheless a marginal recovery of stiffness was notable: 2% and 4% respectively.

When the two components – Nlime and Nsilica solutions – were present in a system of (1 + 1) TETs embedded in the same sample, no strength recovery was recorded and a negligible recovery of stiffness was found. It can therefore be concluded that they failed to trigger any healing mechanisms. Specimens containing 2 TETs, one filled with SS and the other Nlime, achieved positive healing results – even if marginally lower than in samples containing TETs filled with only SS - (Fig. 9 (b)), with strength and stiffness recovery indices of 14% apiece. When comparing samples with 2 TETs filled with SS with samples in which one TET is filled with SS and the other with Nsilica (Fig. 9 (c)), the strength recovery of the latter is slightly lower (16%), whilst the stiffness recovery is significantly higher (39%). Nsilica particles are known to act as nucleation sites for C-S-H gel growth during cement hydration [54] - [55]. In the presence of liquid SS and calcium hydroxide on the crack face, C-S-H may have formed in the crack plane. Whilst the strength of the C-S-H layer may have been low, its presence nonetheless had an impact on the stiffness. Moreover, Nsilica compounds act as a filler, which contributes to the effects of friction and tortuosity along crack surfaces with a consequent stiffness improvement.

4.3. Group 3_Results

The presence of d-TETs, placed in the centre third of the concrete prism and fixed to the bottom via concrete spacers, had a similar performance to that previously seen in samples containing empty d-TETs in Group_1, in so much that the use of SS or SS and Nsilica in the d-TETs had no influence on the general mechanical response, as can be seen in Table 5 and Fig. 10 (a-d). On the con-

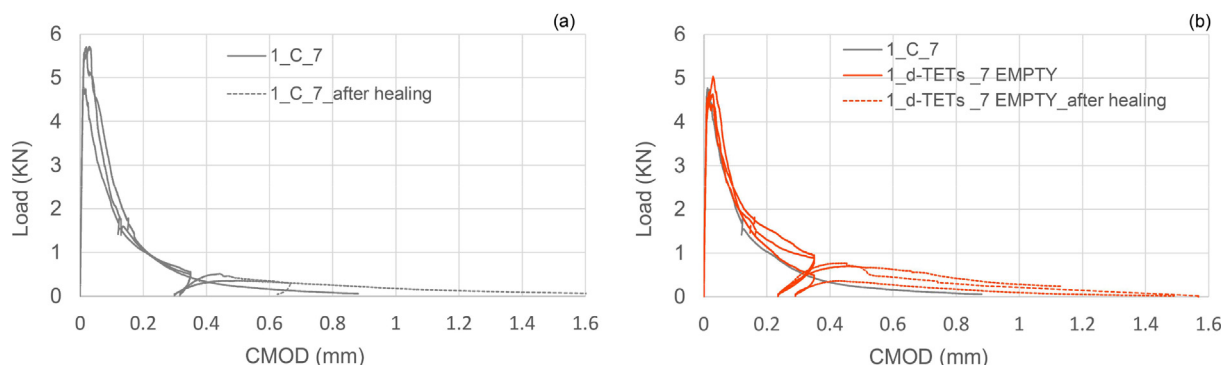


Fig. 7. Flexural load -CMOD response of (a) control specimens after 1 damage-healing cycle and (b) specimens containing empty d-TET after 14 days.

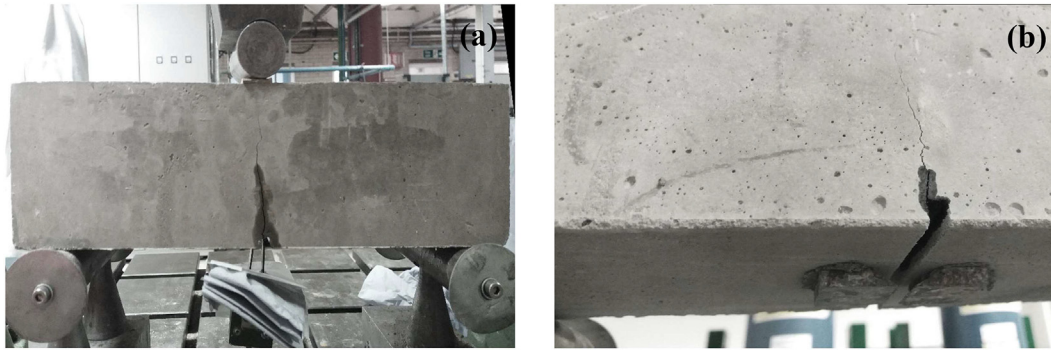


Fig. 8. Evidence of d-TET breakage (a) CMOD of 0.3 mm and (b) CMOD of 0.35 mm.

Table 4

Group_2: Flexural test results and indices of healing.

Group_2	Healing				
	$\sigma_{undamaged}^{k-7}$ MPa (CoV%)	$\sigma_{damaged}^{k-7}$ MPa (CoV%)	σ_{healed}^{k-21} MPa (CoV%)	η_{s-21}^k %	η_{E-21}^k %
2_TETs_7_SS	3.30(5)	0.41(10)	0.93(12)	18	25
2_TETs_7_Nlime	2.79(15)	0.65(13)	0.62(18)	0	2
2_TETs_7_Nsilica	3.56(3)	0.41(25)	0.36(12)	0	4
2_TETs_7_Nsilica_Nlime	2.84(6)	0.62(12)	0.41(2)	0	1
2_TETs_7_SS_Nlime	3.34 (4)	0.68(8)	1.04(14)	14	14
2_TETs_7_SS_Nsilica	3.48(7)	0.64(11)	1.09(6)	16	39

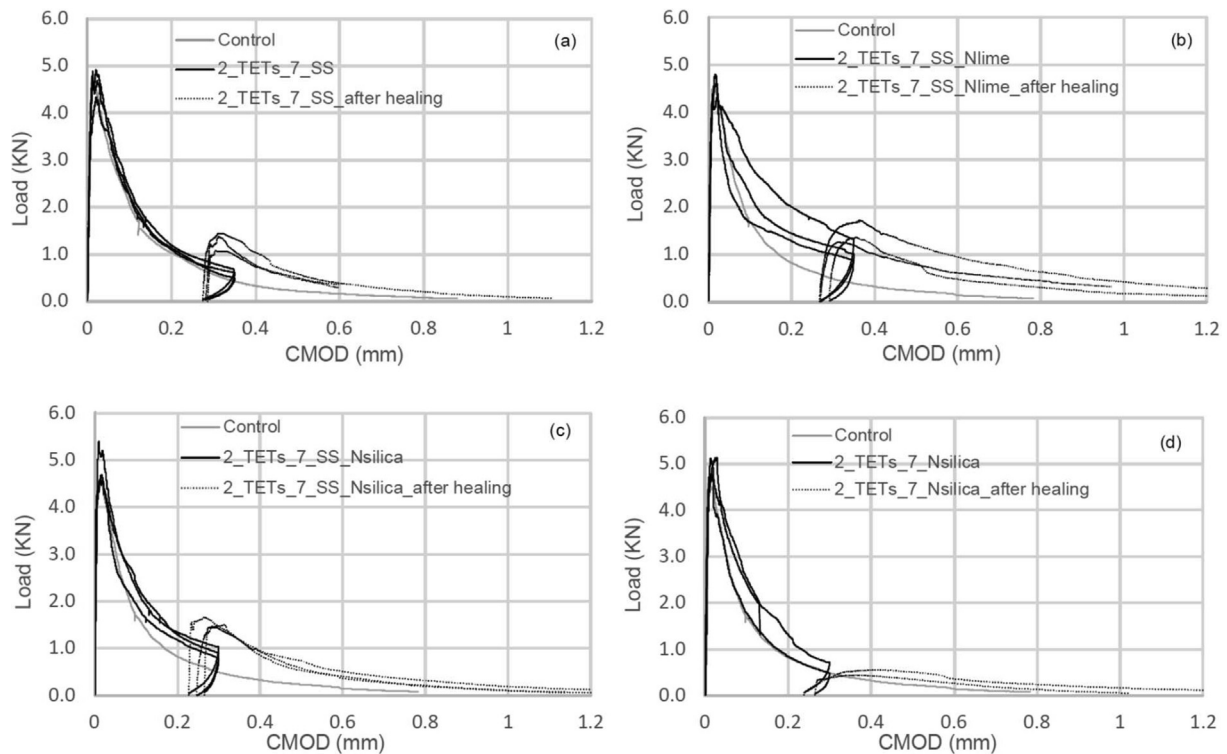


Fig. 9. Group_2: Flexural load-CMOD response for specimens containing (a) 2 TETs filled with SS; (b) 2 TETs filled with SS and Nlime; (c) 2 TETs filled with SS and Nsilica; (d) 2 TETs filled with Nsilica.

rary, the initial flexural strength seems to decrease further (~16%) when the d-TETs are filled with a bicomponent epoxy resin, and furthermore when the d-TETs are filled with SS and Nlime (~23%). A similar flexural strength reduction was observed in samples containing 2 single channel TETs filled with Nlime in Group_2.

In terms of healing efficacy, samples containing d-TETs filled with SS exhibited a similar strength recovery as single channel TETs (17%), but with a higher stiffness recovery in the former (36%). When the SS is used in combination with Nlime and Nsilica dispersions, the strength recovery reached 25% and 20%, whilst the

stiffness recovery was 38% and 40% respectively. It is assumed that the simultaneous presence of Nlime and SS at the time of damage has promoted the formation of C-S-H and led to an enhanced healing performance (+8% in terms of strength recovery, with respect to SS alone). Moreover, the presence of the Nsilica on the crack surface may provide a filler effect, which contributes to the increase in the interfacial adhesion (+14% in terms of strength recovery), as represented in Fig. 10 (c).

d-TETs filled with SS and either Nlime or Nsilica performed better than two single channel TETs containing the same solutions, proving that the simultaneous presence of both components in the right proportions, at the time and location of damage - determined by the rupture of both the d-TET channels- enhances the interaction between the solutions, hence improving the chemical reaction and formation of healing products.

Previous investigations of self-healing performance using sodium silicate solution pumped into continuous vascular networks for 28 days observed a flexural strength recovery of circa. 20% when 1D and 2D vascular networks were used, rising to 34% in 3D vascular network specimens [29]. Recent studies on glass tubular capsules filled with sodium silicate solution showed a flexural strength recovery in a range of 20–25% [56].

In this light, an estimated d-TET flexural strength recovery of 25% is considered promising, on the basis of relatively small quantities of healing agents (8000 mm³ sodium silicate and 1600 mm³ nanolime) being used and taking into account that d-TETs can be readily deployed within a concrete mix without increasing the manufacturing time.

Samples containing epoxy resin showed no healing evidence, as can be seen in Fig. 10 (d). Both epoxy components were of low viscosity and mild hydrophilicity, which implied that there should be no barrier to their flow into a partially saturated crack. Thus, it would seem likely that these unsuccessful results are due to either poor mixing of the two components within the crack or sub-optimal compound mix ratios being achieved on the crack surface.

4.4. Visual observations, digital microscopy and SEM/EDS analyses

In order to provide a deeper insight into the proposed technology, digital micrography was carried out on empty d-TETs after the printing process and on the crack surfaces at the end of the healing cycles SEM analyses were carried out on fragments collected from the crack surfaces to characterise the nature of healing products.

The optimization of the 3D printing process, as described in Section 2.1, ensured a reasonable printing time whilst maintaining a consistent accuracy in layer construction and form. Moreover, the good inter-layer adhesion successfully created impermeable MVN units (Fig. 11 (a)). The 3D printed surface profile on the external d-TET channel coupled with the rib design resulted in a rough surface from which a good bond with the cementitious matrix was achieved. No debonding of the d-TET unit was observed at any stage of the testing programme, as may be seen in Fig. 11 (b-c). Fig. 11 (a) shows the digital micrography of a d-TETs unit after printing; the crack surface at the end of healing cycle in sample

containing d-TETs_SS_Nlime and in sample containing d-TETs_SS_Nsilica can be seen in Fig. 11 (b-c) respectively. At the end of the test, the average distance between the first broken ligaments of d-TETs and the bottom of the prisms was recorded as 12 mm and 14 mm, and the expansion area of healing agent on the crack surface was approximately 55% and 56% for samples containing d-TETs_SS_Nlime and d-TETs_SS_Nsilica respectively (Fig. 10 (b-c)). Further images representing the distribution of the various healing agents over the crack surface are reported in Appendix A.

Following the healing period in the samples containing SS and Nlime, a residual solidified compound was found in the external channel of the d-TET (Fig. 12 (a)) whilst a spread of white crystals can be seen on the crack face in the vicinity of the d-TET ligaments. The former indicates that a single damage-healing cycle fails to consume the entire volume of SS stored within the d-TET and thus remains available for a further damage-healing cycles, as observed in previous experimental investigations [30]. A more detailed examination of the crack surface at the bottom of the prisms (see detail A in Fig. 12 (b)) revealed the presence of a ~ 57 μm thick layer of crystal on the concrete surface, measured across the crystal deposition at point 1 in Fig. 12 (c). The morphology of the crystals suggests the formation of new calcium carbonate [57].

Further microstructural observations on the deposition of healing products within the cementitious matrix were performed using SEM/EDS on the crack surface adjacent to the d-TET (see position 1 in Fig. 11(b)). Representative SEM/EDS images following the healing period are shown in Fig. 13 (a-c). Healing products of varying morphology and dimensions were observed. Crystal deposition, promoted by the presence of Nlime particles, took the form of square plate-like shapes with dimensions ranging between 5 and 15 μm, with occasional agglomerative clusters approximately 40 μm long, see Fig. 13 (b). The main chemical elements of the healing products were Si, Ca, Al, Na as represented in Fig. 13 (c). X-ray elemental maps revealed a significant presence of Si and Ca in distinct, non-overlapping areas on the fracture surface (Fig. 13 (d-f)). The Ca/Si and Na/Si module ratios of the healing products formed in Pos1 were found to be 0.80 and 0.25 respectively, indicating the formation of C-S-H as reported previously by Huang et al [21].

Fibrous healing products were observed around the crack surface, an example is represented in Fig. 14 (a), EDS analysis revealed the presence of Si, Ca, Al, Mg and S, whilst the X-ray elemental maps showed a more homogeneous distribution of Si and Ca. Here the Ca/Si and Na/Si module ratios were found equal to 1.01 and 0.48 respectively. It should be noted that whilst some microcracking may be formed during the sample vacuuming process for image analysis, the microcracks are more evident in the parts where the ratio Ca/Si is low (see Fig. 13 (b)), in line with previous studies [21].

Visual observation of the crack surface of the sample containing d-TETs filled with SS and Nsilica revealed solidified residual compounds in both external and internal channels, as can be seen in Fig. 15 (a). Copious quantities of reacted healing material were also

Table 5
Group_3: Flexural test results and indices of healing.

Group_2	Healing				
	$\sigma_{undamaged}^{k,7}$ MPa (CoV%)	$\sigma_{damaged}^{k,7}$ MPa (CoV%)	$\sigma_{healed}^{k,21}$ MPa (CoV%)	$\eta_{s,21}^k$ %	$\eta_{E,21}^k$ %
3_ d-TETs _7_SS	3.41(11)	0.41(10)	0.92(13)	17	36
3_ d-TETs _7_SS_Nlime	2.89(4)	0.48(28)	1.07(17)	25	38
3_ d-TETs _7_SS_Nsilica	3.20(8)	0.47(38)	0.91(20)	20	40
3_ d-TETs _7_SS_Epoxy	3.15(16)	0.34(20)	0.33(27)	0	0

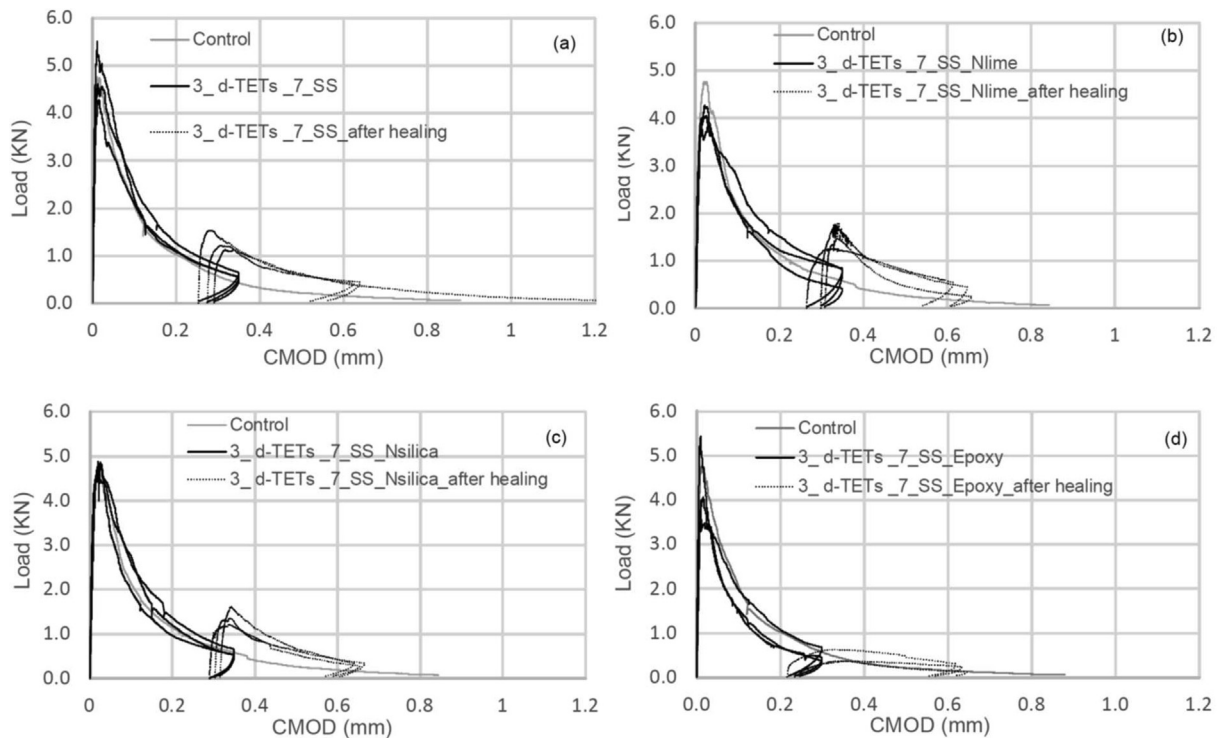


Fig. 10. Group_3: Flexural load-CMOD response for specimens containing (a) d-TETs filled with SS; (b) dTETs filled with SS and Nlime; (c), d-TETs filled with SS and Nsilica and (d) d-TETs filled with epoxy resin.

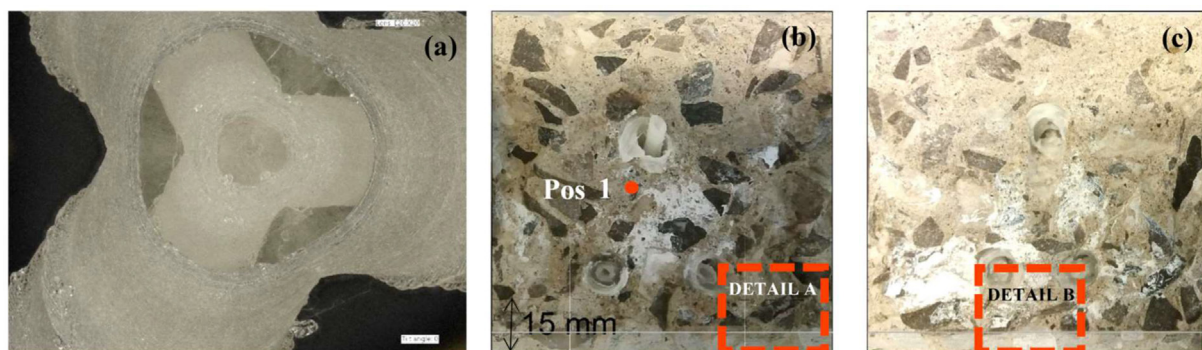


Fig. 11. Digital micrography of a d-TETs unit after printing (a); Crack surface in sample containing dTETs_SS_Nlime (b); in sample containing d-TETs_SS_Nsilica, (c).

deposited in the region of the crack surface closest to the d-TET ligaments (see Fig. 15 (b)), where tightly packed crystals were found, forming $\sim 700 \mu\text{m}$ depth clusters. These deposits, similar to inactive nano-silica particles, might play a filling role, causing a reduction of pore volume, as highlighted by Zhuang et al [58].

4.5. Polymer characterization: Differential scanning calorimetry (DSC)

In order to characterise the PLA polymer and establish any detrimental effect on the polymer from the printing or encapsulation process, DSC and TGA analysis were performed on fragments collected from the filament roll before the printing phase and from the d-TETS immediately after printing and after the healing period. The thermal properties of PLA samples were investigated by DSC analysis, the TGA curves from which are presented in Fig. 16. The pure clear PLA filament showed a thermogram (curve 1) typical of the polymer [59], suggesting the absence of significant quantities of additives and co-polymers, whose presence may interfere with the typical behaviour of the PLA. Thermogram curves

obtained from 3D printed d-TETs (curve 2) highlighted a displacement of the peak of crystallization at higher temperature (from 108°C to $128\text{--}130^\circ$). Furthermore, the measurements showed an even more evident displacement of the melting point from 177°C to $153\text{--}154^\circ\text{C}$, which suggests a change in crystallinity of the polymer and a probable degree of degradation of the polymer itself due to the 3D printing process [59]. Additional calibration and enthalpy measurements would be required in future studies to confirm this. Both crystallization and melting enthalpies seemed not to be significantly affected by the embedment of the d-TET within the cementitious matrix, as represented in curves 3–4. Moreover, no clear variations of the glass transition temperature are evidenced by the thermogram (curves 1–4 $T_g = 58\text{--}59^\circ\text{C}$), thus suggesting no relevant modification of the polymer structure has occurred by either the 3D process or contact with the cementitious matrix. On the contrary, clear changes in T_g temperatures due to contact with SS, Nlime and Nsilica can be seen in curves 5–7, where a T_g displacement in the range of $52\text{--}55^\circ\text{C}$ is highlighted. This indicates a certain modification to the polymer structure induced by

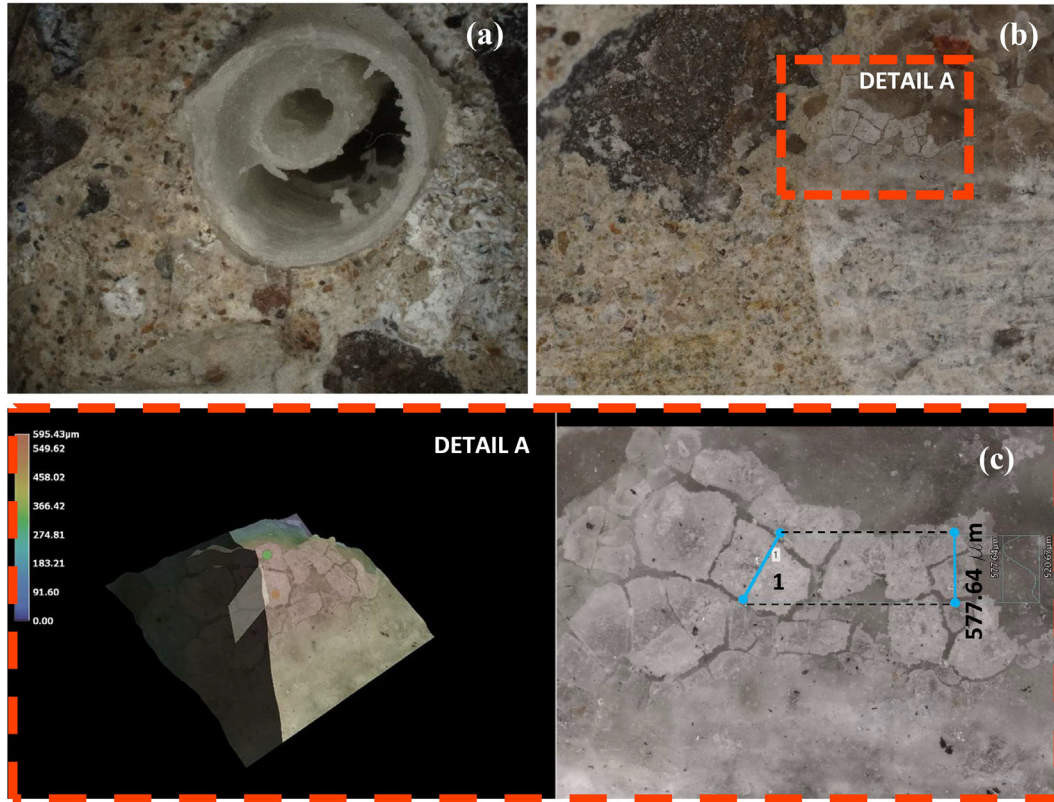


Fig. 12. Micrographies of a sample containing d-TETs_SS_Nlime: d-TETs' ligament detail (a); presence of crystals closes to d-TETs' ligaments (b); morphology of white crystal, detail A (c).

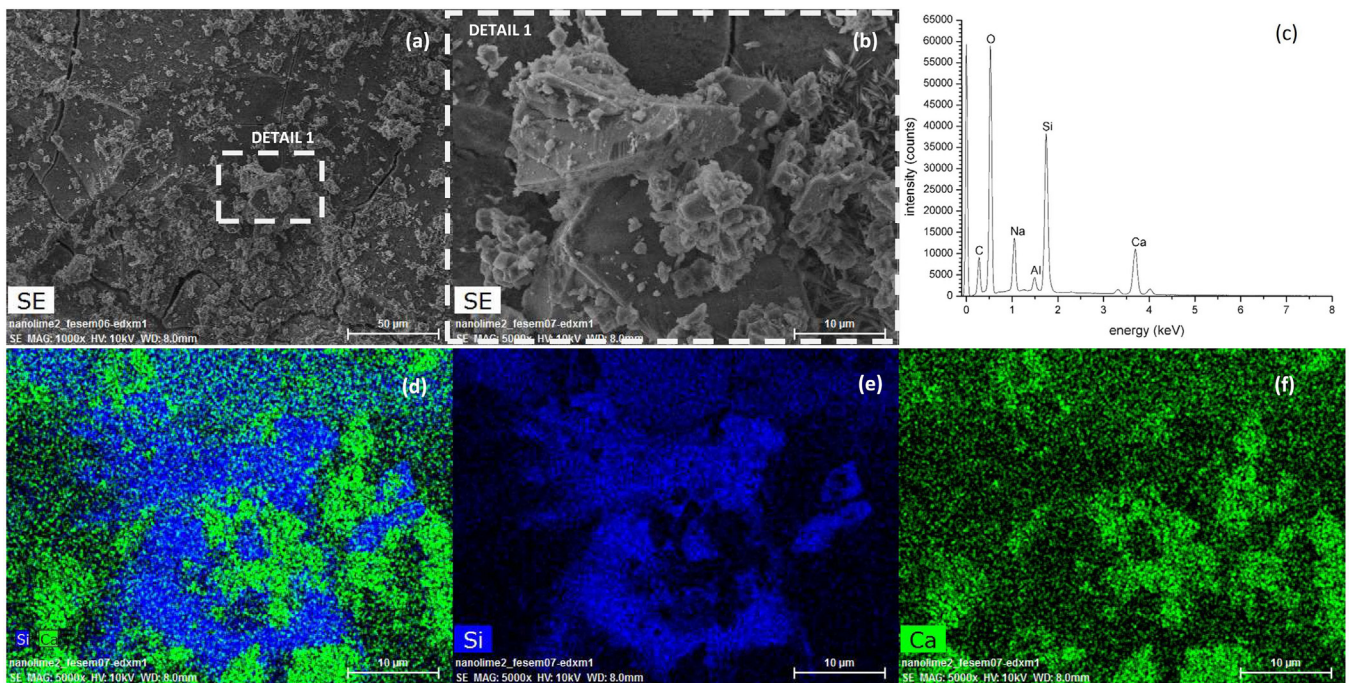


Fig. 13. Various SEM images from the fracture surface of sample containing (a) d-TETs_SS_Nlime; (b) Magnification of (a); (c) EDS output (d) X-ray (EDX) elemental maps for Si-Ca; (e) X-ray (EDX) elemental maps for Si and (f) X-ray (EDX) elemental maps for Ca at point in DETAIL 1.

the presence of alkaline healing agents, whose adsorption onto the polymer surface may influence such a physical property. SS, Nlime and Nsilica are all suspensions of particles in water or solvents, and the latter is a known to cause degradation of the polymer when it

comes into direct contact. In particular, the presence of isopropyl alcohol in Nlime solution might have also caused transesterification reactions which may have increased further the material degradation [60].

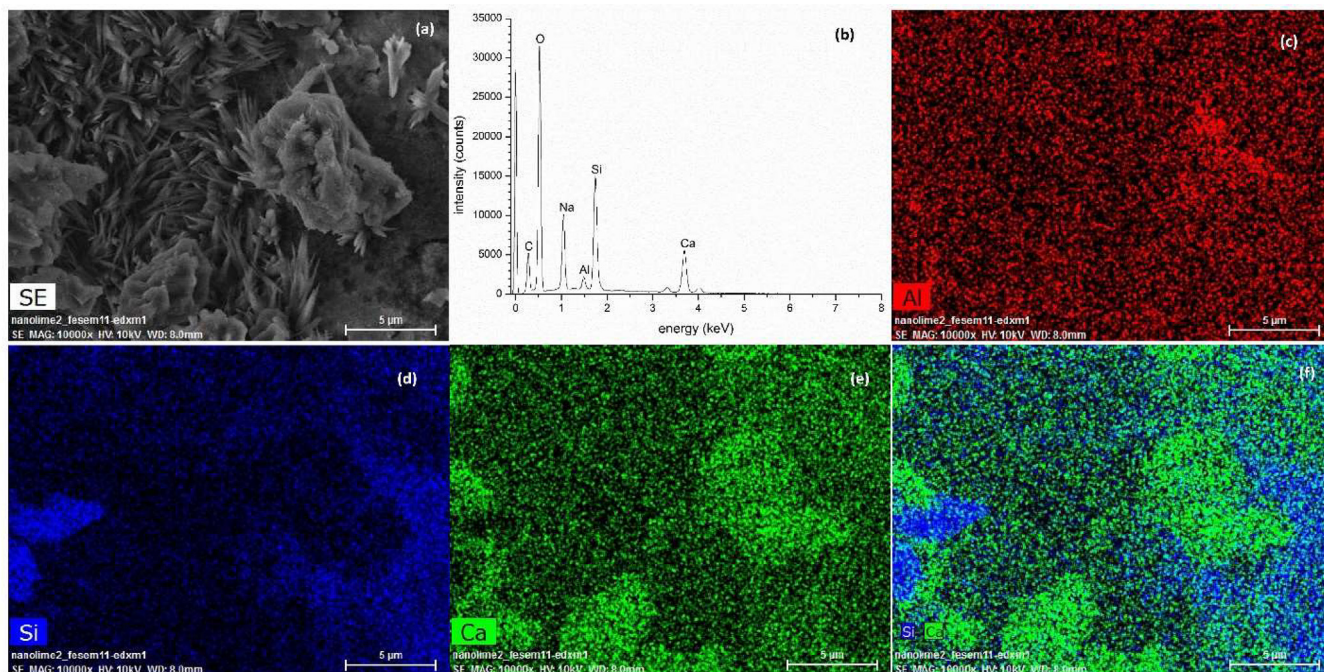


Fig. 14. SEM images from the fracture surface of sample containing (a) d-TETS_SS_Nlime; (b) EDS output; (c) X-ray (EDX) elemental maps for Al; (d) X-ray (EDX) elemental maps for Si; (e) X-ray (EDX) elemental maps for Ca and (f) X-ray (EDX) elemental maps for Si + Ca.

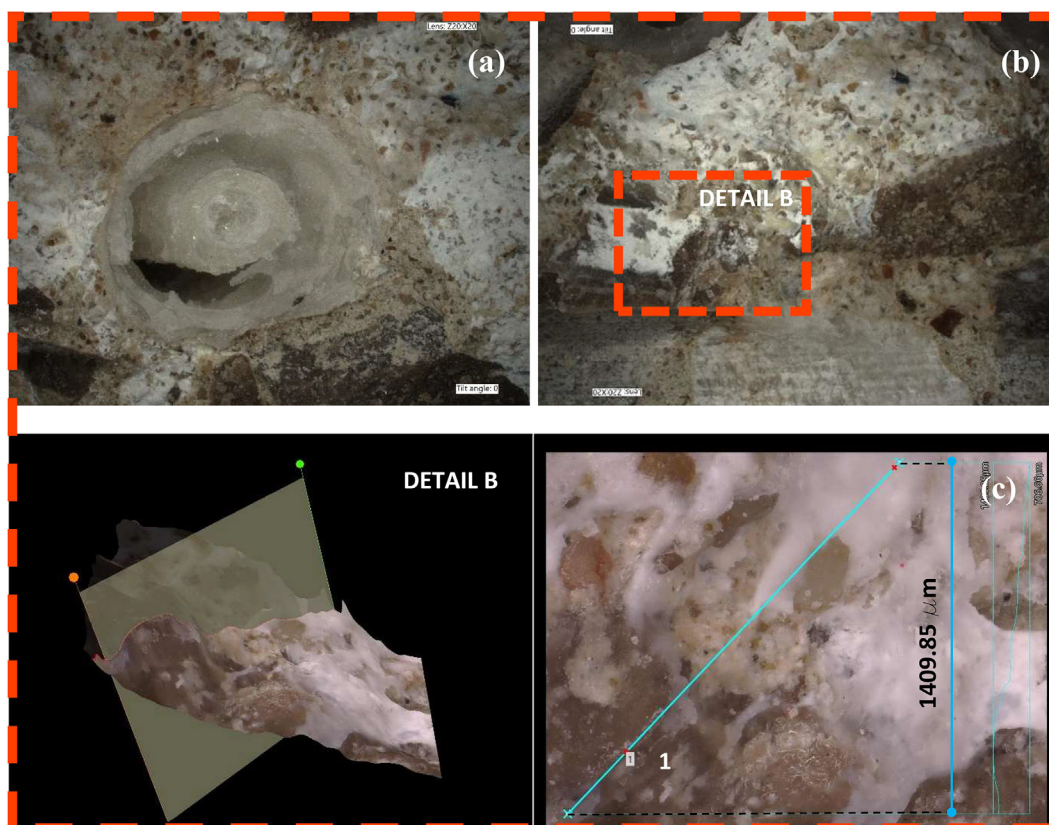


Fig. 15. Micrographies of a sample containing d-TETS_SS_Nsilica: (a) d-TETS' ligament detail (a); presence of crystals (b); morphology of white crystal, detail B (c).

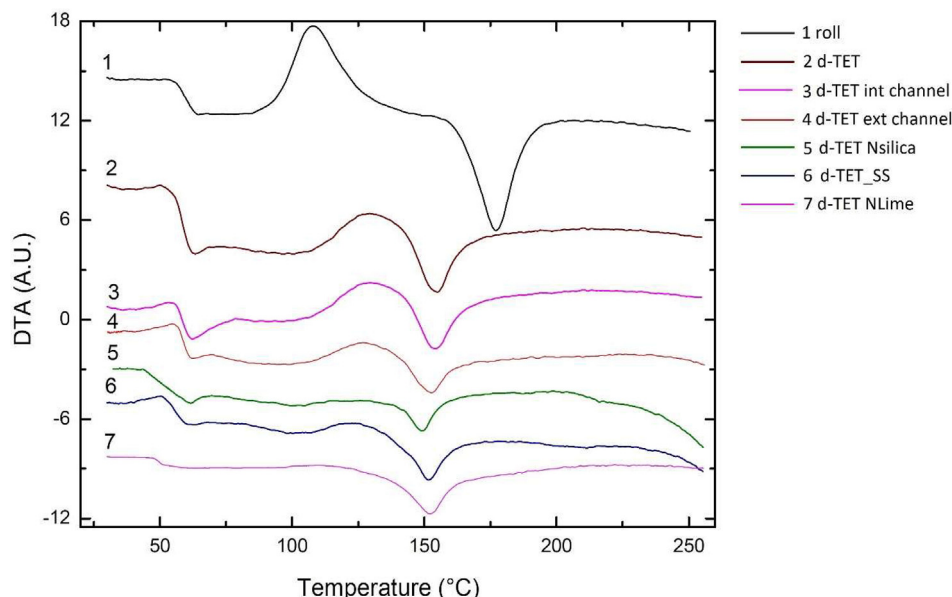


Fig. 16. DSC measurements of various PLA samples obtained from TETS in different conditions recovered inside the specimen used in mechanical evaluation. Run conditions: open aluminium crucible, sample 40 mg, ramp 10 °C/min to 250 °C, nitrogen flow 80 mL/min.

5. Conclusions

In this research a form of biomimetic cementitious material, which employs novel dual channel PLA 3D printed mini-vascular networks (d-TETs) to store and deliver healing agents to damage sites within cementitious matrices has been investigated. The d-TET ligaments are formed from dual co-axial hollow channels which allows for the first time the storage of bi-component healing agents. Different healing agents were selected following consideration of their flow properties and mechanical behaviour. Two strategies for this were adopted, firstly agents which would further enhance the healing ability of sodium silicate (SS) healing efficiency, i.e Nanolime (Nlime) and Nanosilica (Nsilica) solutions, and secondly the use of an existing and commercially available bi-component healing agent (Epoxy).

Preliminary tests were performed to optimize the d-TET design and 3D printing process to fulfil the design criteria, namely i) the ability to host the two components in a dormant state and without premature mixing, ii) the ability to be fully watertight when embedded into a cementitious matrix, iii) rupture at a defined level of damage. The healing efficacy was evaluated by means of a three-point bend test and samples containing d-TETs filled with either a commercially available bi-component epoxy resin, sodium silicate ($\text{Na}_2\text{O}_3\text{Si}$) solution and nanolime (CaOH_2) or Nanosilica solution were compared with control samples and samples containing the same solutions stored in single channel TETs. Light microscopy coupled with SEM/EDS analysis were performed on samples collected from the crack surface. TGA and DSC analyses were carried out on the d-TET PLA polymer before and after the healing period.

From the analyses of the results presented in the paper, the following main conclusions can be drawn:

- the new MVN design (d-TET) allowed the potentially short shelf life of single-component healing agent to be overcome. The d-TET, manufactured from PLA, has a flexible design, capable of storing bi-component healing agents in differing volume ratios without premature mixing and curing.
- d-TETs, even when empty, act as reinforcement and have negligible impact on the 28-day strength of the concrete mix. The 3D printed pattern coupled with the rib design showed good bond

between the d-TET ligaments and the concrete matrix, ensuring that the coaxial channels ruptured at a crack width typical of in-situ serviceability limit state crack (0.35 mm).

- d-TETs filled simultaneously with SS and either Nlime or Nsilica showed representative strength and stiffness recovery indices of 25%, 38% and 20%, 40% respectively. Both indices of healing have been improved in comparison to samples containing only SS as healing agent (17%, 36%). The same healing agents stored individually within single channel TETs had lower performance, SS + Nlime can produce strength and stiffness recoveries of 14% and 14% respectively, whilst SS + Nsilica showed a recovery of 16 and 39% respectively. This confirms the beneficial effect of the concurrent release of both components at the time of damage.
- samples containing d-TETs filled with a bi-component epoxy, showed no evidence of healing. The polymerisation reaction may not have taken place due to an incorrect stoichiometry ratio or lack of adequate mixing of components in the crack plane.
- SEM/EDS analysis carried out on samples collected from the crack surface highlighted the presence of the main chemical elements forming C-S-H. Different crystal depositions found on the crack surface suggested the promotion of healing through the reaction of sodium silicate and Nlime.
- DSC analysis carried out on PLA samples highlighted that the most relevant polymer changes occurred as a result of the quite complex 3D printing process which is needed to manufacture the d-TET. No evidence of polymer degradation due to its embedment in the concrete matrix was observed. Light changes in glass transition temperature (T_g) were found in samples collected from channels filled with SS, Nsilica and Nlime, with the Nlime solution causing the highest changes in the polymer.

In summary, d-TETs form the basis of a viable self-healing system for concrete, able to protect separately two healing agents for a sufficient period of time and release them at design crack size. The research presented herein has developed new approach which encompasses the simultaneous storage of a healing agent and an enhancer of healing, that will be available at the time of damage in the vicinity of any crack. The successful encapsulation and

release at serviceability level crack widths demonstrate the system's potential to address a wide variety of damage whilst being easily incorporated into a concrete mix in a real-world application.

Poly(lactic acid) (PLA) is the most widely used commercial bio-based plastic, derived from 100% renewable resources. It has good mechanical properties for manufacturing 3D printed MVNs. However, when PLA is in contact with alkaline liquids and solvents, it has a tendency to degrade over time. The next stage of the research will explore the potential to treat PLA surfaces in order to improve its chemical resistance.

On-going research is also exploring different MVNs shapes and dimension, alternative thermoplastic polymers as well as new formulation of healing agents with an improved encapsulation stability and a range of trigger mechanisms for curing. As part of this on-going research, a coupled finite element model [61] is being used as a predictive tool to guide the physical testing and narrow down the parameter space.

Funding

This research was funded by the Engineering and Physical Sciences Research Council (EPSRC), grant number EP/P02081X/1.

CRediT authorship contribution statement

Cristina De Nardi: Conceptualization, Methodology, Formal analysis, Data curation, Investigation, Validation, Writing - original draft, Writing - review & editing. **Diane Gardner:** Conceptualization, Supervision, Funding acquisition, Project administration, Writing - review & editing. **Davide Cristofori:** Formal analysis, Data curation. **Lucio Ronchin:** Formal analysis, Data curation. **Tony Jefferson:** Conceptualization, Supervision, Project administration, Funding acquisition, Writing - review & editing.

Data availability

Information on the data underpinning the results presented here, including how to access them, can be found at Cardiff University data catalogue at [DOI XXX to be confirmed prior to publication].

Declaration of Competing Interest

The authors declare the following financial interests/personal relationships which may be considered as potential competing interests: Cristina De Nardi reports financial support was provided by Engineering and Physical Sciences Research Council. Diane Gardner reports financial support was provided by Engineering and Physical Sciences Research Council. Antony Jefferson reports financial support was provided by Engineering and Physical Sciences Research Council.

Acknowledgement

This research was funded by the Engineering and Physical Sciences Research Council (EPSRC), grant number EP/P02081X/1. The Authors would like to thank KEYENCE for the microscopy analysis. The authors would also like to acknowledge the considerable help and expertise of Richard Thomas, Ian King and Carl Wadsworth without whom the laboratory work would not have been possible. Thanks also to both Samuel Moeller for his technical support on 3D printing and Giulia Cazzador for her support on PLA polymer analyses. Information on the data underpinning the results presented here, including how to access them, can be found

at Cardiff University data catalogue at <http://doi.org/10.17035/d.2023.0252931383>.

Appendix A. Supplementary data

Supplementary data to this article can be found online at <https://doi.org/10.1016/j.matdes.2023.111939>.

References

- [1] W. M. C., K. Dirk, Biomimicry and Structural Design: Past, Present, and Future, *Struct. Cong.* (2010) 2852–2863, doi: 10.1061/41130(369)258.
- [2] P. Saha, Biomimicry and its adaptations to solve complex problems in civil engineering system, in: *ICSCI 2014*, 2015, no. August, pp. 942–951.
- [3] D. Gardner, R. Lark, T. Jefferson, R. Davies, A survey on problems encountered in current concrete construction and the potential benefits of self-healing cementitious materials, *Case Stud. Constr. Mater.* 8 (2018) 238–247, <https://doi.org/10.1016/j.cscm.2018.02.002>.
- [4] M.R. Hossain, R. Sultana, M.M. Patwary, N. Khunga, P. Sharma, S.J. Shaker, Self-healing concrete for sustainable buildings. A review, *Environ. Chem. Lett.* 20 (2) (2022) 1265–1273, <https://doi.org/10.1007/s10311-021-01375-9>.
- [5] N. De Belie, K. Van Tittelboom, M. Sánchez Moreno, L. Ferrara, E. Gruyaert, Self-Healing Concrete Research in the European Projects SARCOS and SMARTINCS BT - Proceedings of the 3rd RILEM Spring Convention and Conference (RSCC 2020), 2022, pp. 303–307.
- [6] N. De Belie et al., A Review of Self-Healing Concrete for Damage Management of Structures, *Adv. Mater. Interfaces* 5 (17) (Sep. 2018) 1800074, <https://doi.org/10.1002/admi.201800074>.
- [7] C. Edvardsen, Water Permeability and Autogenous Healing of Cracks in Concrete, *ACI Mater. J.* 96(4), doi: 10.14359/645.
- [8] M.R. de Rooij, K. Van Tittelboom, N. De Belie, E. Schlangen, Self-healing phenomena in cement-based materials, 2013.
- [9] E. Tsangouri, C. Van Loo, Y. Shields, N. De Belie, K. Van Tittelboom, D.G. Aggelis, Reservoir-Vascular Tubes Network for Self-Healing Concrete: Performance Analysis by Acoustic Emission, Digital Image Correlation and Ultrasound Velocity, *Appl. Sci.* 12 (10) (2022), <https://doi.org/10.3390/app12104821>.
- [10] R. Maddalena, L. Bonanno, B. Balzano, C. Tuinea-Bobe, J. Sweeney, I. Mihai, A crack closure system for cementitious composite materials using knotted shape memory polymer (k-SMP) fibres, *Cem. Concr. Compos.* 114 (2020), <https://doi.org/10.1016/j.cemconcomp.2020.103757> 103757.
- [11] E. Tsangouri et al., Feasibility study on real-scale, self-healing concrete slab by developing a smart capsules network and assessed by a plethora of advanced monitoring techniques, *Constr. Build. Mater.* 228 (2019), <https://doi.org/10.1016/j.conbuildmat.2019.116780> 116780.
- [12] C. Dry, W. McMillan, Three-part methylmethacrylate adhesive system as an internal delivery system for smart responsive concrete, *Smart Mater. Struct.* 5 (3) (1996) 297–300, <https://doi.org/10.1088/0964-1726/5/3/007>.
- [13] A. Beglarigale, N. Yag, Sodium silicate / polyurethane microcapsules used for self-healing in cementitious materials : Monomer optimization , characterization , and fracture behavior 162 (2018) 57–64, doi: 10.1016/j.conbuildmat.2017.11.164.
- [14] H. Dong, H. Huang, G. Ye, Inorganic powder encapsulated in brittle polymer particles for self-healing cement-based materials, in: *ICSHM 2013: Proceedings of the 4th International on Self-Healing Materials, Ghent, Belgium, 16-20 June 2013*, pp. 123–128.
- [15] A. Pelletier, M. Brown, R. Shukla, A. Bose, Self-healing concrete with a microencapsulated healing agent, 2011.
- [16] C. Xue, W. Li, A review study on encapsulation-based self-healing for cementitious materials, no. July 2018 (2019) 198–212, doi: 10.1002/suco.201800177.
- [17] V.C. Li, Y.M. Lim, Y.W. Chan, Y. Mook, Y.W. Chan, Feasibility study of a passive smart self-healing cementitious composite, *Compos. Part B. Eng.* 29 (6) (1998) 819–827, [https://doi.org/10.1016/S1359-8368\(98\)00034-1](https://doi.org/10.1016/S1359-8368(98)00034-1).
- [18] B. Hilloulin, K. Van Tittelboom, E. Gruyaert, N. De Belie, A. Loukili, Cement & Concrete Composites Design of polymeric capsules for self-healing concrete, *Cem. Concr. Compos.* 55 (2015) 298–307, <https://doi.org/10.1016/j.cemconcomp.2014.09.022>.
- [19] L. Souza, A. Al-tabbaa, Microfluidic fabrication of microcapsules tailored for self-healing in cementitious materials Microfluidic fabrication of microcapsules tailored for self-healing in cementitious materials, *Constr. Build. Mater.* 184 (September) (2018) 713–722, <https://doi.org/10.1016/j.conbuildmat.2018.07.005>.
- [20] K. Van Tittelboom, K. Adesanya, P. Dubruel, P. Van Puyvelde, N. De Belie, Methyl methacrylate as a healing agent for self-healing cementitious materials, *Smart Mater. Struct.* 20 (12) (2011), <https://doi.org/10.1088/0964-1726/20/12/125016> 125016.
- [21] H. Huang, G. Ye, Application of sodium silicate solution as self-healing agent in cementitious materials, no. 1993, 2011.
- [22] A. Kalagri, A. Miltiadou-Fezans, E. Vintzileou, Design and evaluation of hydraulic lime grouts for the strengthening of stone masonry historic structures, *Mater. Struct. Constr.* 43 (8) (2010) 1135–1146, <https://doi.org/10.1617/s11527-009-9572-1>.

- [23] K. Van Tittelboom et al., Comparison of different approaches for self-healing concrete in a large-scale lab test, *Constr. Build. Mater.* 107 (2016) 125–137, <https://doi.org/10.1016/j.conbuildmat.2015.12.186>.
- [24] R.S. Trask, H.R. Williams, I.P. Bond, Self-healing polymer composites: mimicking nature to enhance performance, *Bioinspir. Biomim.* 2 (1) (Jan. 2007) P1–P9, <https://doi.org/10.1088/1748-3182/2/1/p01>.
- [25] B. Blaiszik, S. Kramer, S. Olugebefola, J. Moore, N. Sottos, Self-Healing Polymers and Composites, *Annu. Rev. Mater. Res.* 40 (2010) 179–211211, <https://doi.org/10.1146/annurev-matsci-070909-104532>.
- [26] C. Joseph, A.D. Jefferson, B. Isaacs, R. Lark, D. Gardner, Experimental investigation of adhesive-based self-healing of cementitious materials, *Mag. Concr. Res.* 62 (11) (2010) 831–843, <https://doi.org/10.1680/macrc.2010.62.11.831>.
- [27] C. Joseph, A. Jefferson, and M. Cantoni, "Issues relating to the autonomic healing of cementitious materials," Proceedings of the First International Conference on Self Healing Materials, 2007, Noordwijk aan Zee, The Netherlands [<https://studylib.net/doc/14915396/issues-relating-to-the-autonomic-healing-of-cementitious-...>].
- [28] A. Pareek, S. Oohira, A fundamental study on regain of flexural strength of mortars by, in: *3rd International Conference on Self Healing Materials, 696 Bath, UK*, 2011, no. June, pp. 1–2.
- [29] Z. Li, L.R. De Souza, C. Litina, A.E. Markaki, A. Al-Tabbaa, A novel biomimetic design of a 3D vascular structure for self-healing in cementitious materials using Murray's law, *Mater. Des.* 190 (2020) 1–14, <https://doi.org/10.1016/j.matdes.2020.108572>.
- [30] C. De Nardi et al., Experimental Investigation of a Novel Formulation of a Cyanoacrylate-Based Adhesive for Self-Healing Concrete Technologies, *Front. Built Environ.* 7 (2021) 1–15, <https://doi.org/10.3389/fbuil.2021.660562>.
- [31] C. Joseph, D. Gardner, T. Jefferson, B. Isaacs, B. Lark, Self-healing cementitious materials: a review of recent work, *Proc. Inst. Civ. Eng. - Constr. Mater.* 164 (1) (2011) 29–41, <https://doi.org/10.1680/coma.900051>.
- [32] C. Dry, Design of Self-growing, Self-sensing and Self-repairing Materials for Engineering Applications, vol. 4234, 2001, pp. 23–29.
- [33] C. M. Dry, Smart earthquake-resistant materials: using time-released adhesives for damping, stiffening, and deflection control, in: *3rd International Conference on Intelligent Materials and 3rd European Conference on Smart Structures and Materials*, 1996, vol. 2779, pp. 958–967, doi: 10.1117/12.237085.
- [34] S. Senot, E. Schlangen, Self Healing of Concrete Structures - Novel Approach Using Porous Network Concrete, *J. Adv. Concr. Technol.* 10 (5) (2012) 185–194, <https://doi.org/10.3151/jact.10.185>.
- [35] S. Senot, E. Schlangen, V.C. Li, E. Herbert, Self Healing of Concrete Structures - Novel approach using porous network concrete Self Healing of Concrete Structures - Novel Approach Using Porous Network Concrete, vol. 10, 2012, pp. 185–194, doi: 10.3151/jact.10.185.
- [36] R. Davies, D. Gardner, J. Anthony, B. Lark, A novel 2d vascular network in cementitious materials, in: *FIB Proceedings - Concrete - Innovation and Design*, Copenhagen: FIB - Féd. Int. du Béton, 2015.
- [37] C. M. Dry, J. Unzicker, Use of embedded self-repair adhesives in certain areas of concrete bridge members to prevent failure from severe dynamic loading, in: *Proc. SPIE*, Jul. 1999, vol. 3675, doi: 10.1117/12.352786.
- [38] D. Gardner, A. Jefferson, A. Hoffman, R. Lark, Simulation of the capillary flow of an autonomic healing agent in discrete cracks in cementitious materials, *Cem. Concr. Res.* 58 (2014) 35–44, <https://doi.org/10.1016/j.cemconres.2014.01.005>.
- [39] G. Perez, E. Erkizia, G. Jj, I. Kaltzakorta, I. Jimenez, A. Guerrero, Synthesis and characterization of epoxy encapsulating silica microcapsules and amine functionalized silica nanoparticles for development of an innovative self-healing concrete, *Mater. Chem. Phys.* 165 (2015) 39–48, <https://doi.org/10.1016/j.matchemphys.2015.08.047>.
- [40] K. Van Tittelboom, N. De Belie, D. Van Loo, P. Jacobs, Self-healing efficiency of cementitious materials containing tubular capsules filled with healing agent, *Cem. Concr. Compos.* 33 (4) (2011) 497–505, <https://doi.org/10.1016/j.cemconcomp.2011.01.004>.
- [41] M. Maes, K. Van Tittelboom, N. De Belie, The efficiency of self-healing cementitious materials by means of encapsulated polyurethane in chloride containing environments, *Constr. Build. Mater.* 71 (2014) 528–537, <https://doi.org/10.1016/j.conbuildmat.2014.08.053>.
- [42] M. Hirozo, K. Yoshio, N. Tomoya, O. Koji, Fundamental Study on Development of Intelligent Concrete Characterized by Self-Healing Capability for Strength, *Concr. Res. Technol.* 11 (2) (2000) 21–28, <https://doi.org/10.3151/crt1990.11.2.21>.
- [43] M. Ehsan, A. Somayeh, H. M. M., A. Mohamed, Evaluation of Self-Healing Mechanisms in Concrete with Double-Walled Sodium Silicate Microcapsules, *J. Mater. Civ. Eng.*, vol. 27, no. 12, p. 4015035, Dec. 2015, doi: 10.1061/(ASCE)MT.1943-5533.0001314.
- [44] D. Gardner, A. Jefferson, A. Hoffman, Investigation of capillary flow in discrete cracks in cementitious materials, *Cem. Concr. Res.* 42 (7) (2012) 972–981, <https://doi.org/10.1016/j.cemconres.2012.03.017>.
- [45] G. James, H. M. M., R. Tyson, B. Michele, O. Ayman, A. Somayeh, Dicyclopentadiene and Sodium Silicate Microencapsulation for Self-Healing of Concrete, *J. Mater. Civ. Eng.*, vol. 26, no. 5, pp. 886–896, May 2014, doi: 10.1061/(ASCE)MT.1943-5533.0000892.
- [46] Y. Shields, N. De Belie, A. Jefferson, K. Van Tittelboom, A review of vascular networks for self-healing applications, *Smart Mater. Struct.* 30 (6) (2021) pp, <https://doi.org/10.1088/1361-665X/abf41d>.
- [47] C. De Nardi, D. Gardner, A.D. Jefferson, Development of 3D printed networks in self-healing concrete, *Materials (Basel)* 13 (6) (2020) pp, <https://doi.org/10.3390/ma13061328>.
- [48] C. De Nardi, D. Gardner, A. Jefferson, T. Selvarajoo, G. Evans, Durable Concrete for Infrastructure under Severe Conditions. Smart Admixtures, Self-responsiveness and nano additions, in: *Durable Concrete for Infrastructure under Severe Conditions Durable Concrete for Infrastructure under Severe Conditions*, 2019, no. September, pp. 19–23.
- [49] Bresciani, "Bresciani, EP 2101 Eurostac strengthener, Datasheet." pp. 1–5.
- [50] C. Selwitz, *Research in Conservation. Epoxy Resins in Stone Conservation*. 1992.
- [51] E. Tesser, L. Lazzarini, S. Bracci, Investigation on the chemical structure and ageing transformations of the cycloaliphatic epoxy resin EP2101 used as stone consolidant, *J. Cult. Herit.* 31 (2018) 72–82, <https://doi.org/10.1016/j.culher.2017.11.002>.
- [52] D. Homma, H. Mihashi, T. Nishiwaki, Self-Healing Capability of Fibre Reinforced Cementitious Composites, *J. Adv. Concr. Technol.* 7 (2) (2009) 217–228, <https://doi.org/10.3151/jact.7.217>.
- [53] L. Ferrara, V. Krelani, F. Moretti, M. Roig Flores, P. Serna Ros, Effects of autogenous healing on the recovery of mechanical performance of High Performance Fibre Reinforced Cementitious Composites (HPFRCCs): Part 1, *Cem. Concr. Compos.* 83 (2017) 76–100, <https://doi.org/10.1016/j.cemconcomp.2017.07.010>.
- [54] Z. Rong, W. Sun, H. Xiao, G. Jiang, Effects of nano-SiO₂ particles on the mechanical and microstructural properties of ultra-high performance cementitious composites, *Cem. Concr. Compos.* 56 (2015) 25–31, <https://doi.org/10.1016/j.cemconcomp.2014.11.001>.
- [55] D. Kong, S. Huang, D. Corr, Y. Yang, S.P. Shah, Whether do nano-particles act as nucleation sites for C-S-H gel growth during cement hydration?, *Cem Concr. Compos.* 87 (2018) 98–109, <https://doi.org/10.1016/j.cemconcomp.2017.12.007>.
- [56] A. Kanellopoulos, T.S. Qureshi, A. Al-Tabbaa, Glass encapsulated minerals for self-healing in cement based composites, *Constr. Build. Mater.* 98 (2015) 780–791, <https://doi.org/10.1016/j.conbuildmat.2015.08.127>.
- [57] J. Otero, V. Starinieri, A.E. Charola, Nanolime for the consolidation of lime mortars: A comparison of three available products, *Constr. Build. Mater.* 181 (2018) 394–407, <https://doi.org/10.1016/j.conbuildmat.2018.06.055>.
- [58] C. Zhuang, Y. Chen, The effect of nano-SiO₂ on concrete properties: a review, *Nanotechnol. Rev.* 8 (1) (2019) 562–572.
- [59] M. Cuiffo, J. Snyder, A. Elliott, N. Romero, S. Kannan, G. Halada, Impact of the Fused Deposition (FDM) Printing Process on Poly(lactic acid) (PLA) Chemistry and Structure, *Appl. Sci.* 77 (579) (2017) 1–14, <https://doi.org/10.3390/app7060579>.
- [60] F. Iñiguez-Franco et al., Chemical recycling of poly(lactic acid) by water-ethanol solutions, *Polym. Degrad. Stab.*, vol. 149, no. November 2017, pp. 28–38, 2018, doi: 10.1016/j.polymdegradstab.2018.01.016.
- [61] B. L. Freeman, T. D. Jefferson, "A 3D coupled finite element model for simulating mechanical regain in self-healing cementitious materials," *Manuscr. Submitt. Publ.*